ASPECTS OF THE NUMERICAL SIMULATION FOR THE FLOW IN PENSTOCKS

E. Casartelli
HSLU Lucerne
Technikumstrasse 21
CH-6048 Horw
Switzerland

N. Ledergerber
HSLU Lucerne
Technikumstrasse 21
CH-6048 Horw
Switzerland

ABSTRACT

The flow in a full-scale penstock has been computed. Characteristic of this flow is the very high device Reynolds-number, which ranges from up to 100 millions.

The results show that for the numerical simulations special care has to be applied to mesh, boundary conditions, turbulence models and numerics. A good understanding of the models and assumptions involved in the CFD is necessary, especially for the wall function, which is used in order to reduce the wall resolution in the mesh. Recent research results show that the parameters of the law of the wall at high Reynolds numbers change compared to the established values at typical turbulent conditions (device Reynolds-Number up to 1 million).

Standard procedures can therefore lead to an incorrect computation of the wall shear stress, thus strongly affecting the results (pressure drop, velocity profile, secondary flow).

Mesh quality has been identified as a key parameter for this kind of flows. The very low viscosity present in the flow can lead to instabilities, which can be of physical or numerical nature. Both affect the convergence of steady state simulations, thus making a transient approach necessary.
In the paper numerical and physical aspects for this kind of simulations and flows are included.
The numerical data is then evaluated in order to assess the impact of flow distortion on ultrasonic measurements, with the goal to improve the accuracy of the measured integral predictions.

INTRODUCTION

The flow in a full-scale penstock is characterized by a very high device Reynolds-number, which often ranges from 10 to 100 millions. At this regime the boundary-layer behavior is still matter of investigation, and the obtained research results on its structure and characteristics do not present a clear and unique picture. [Marusic 2010] presents a good review on the topic and the latest research results.

In the past ten years the use of CFD at very high Reynolds-number has increased, with different levels of success. One of the applications of such computations is definitely the penstock flow simulation with disturbed conditions [Staubli 2007 and 2008, Adamkowski 2008], as it can be observed behind bends and bifurcations. The secondary-flow leads to a 3D flow structure. This also influences and determines the axial velocity distribution. In certain flow configurations this can even produce unsteady flow pattern.

The flow behavior in these situations needs to be understood in order to assess its impact on the machine performance. On the other hand the results can be used for the optimization of flow metering devices, as for example suggested in the OWISS method [Staubli 2007 and 2008] used in ultrasonic flow metering. In this case the simulation results play a key role in the positioning of the measuring paths and in the choice of the weighting factors.

In the paper aspects of CFD at this regime are presented. The findings are then transferred to the flow metering applications.

CFD NEEDS

Due to the high device Reynolds-number the boundary layer is very thin and the gradients at the wall are extremely high. A first question which arises is how this can be taken into account with everyday CFD.

Three different aspects, which are strongly correlated, are very important here:
- grid size and flow resolution
- computational time
- adequacy of the turbulence and wall models

The grid spacing at the wall needs to be refined accordingly in order to capture the strong gradient in the velocity distribution. This affects directly the computational time, which can increase dramatically.

A well established practice to handle the boundary layer in turbulence models is to use a universal wall function, thus allowing for relatively coarse meshes at the walls, since the boundary layer does not have to be resolved, and so helping to reduce the model size and the computational time.

Even with this kind of approach, the grid sizes reach the order of magnitude of 10 millions cells, making this kind of computations highly time consuming.

As stated in the introduction, one of the major focuses in the boundary layer research at high Reynolds-number is its characterization, including the impact on the law of the wall. It seems that at this regime the overall behavior is still similar to that at lower Re-numbers (e.g. 50’000 to 500’000), but that the different ranges in which the boundary layer is subdivided are shifted to higher values of y+ (dimensionless wall distance) and that the constants in the log-law of the wall may vary from the established values [Marusic 2010]. This implies that the choice of a standard wall function can be a source of uncertainty. In order to avoid an overestimation of the wall shear- stress a relatively large y+ (200 .. 500) should be used, when working with a wall function with a standard log-law.

Moreover the choice of the turbulence model is also important. The models mainly used in industrial CFD are two-equation turbulence models, such as k-□ and k-□ models or combinations of them like the SST Model [Menter 1994]. Since turbulence structure at the high Re regime is not well understood, it is difficult to assess the effects of the assumption of an isotropic turbulence, which is at the base of two-equation models.

Knowing this, a short review of the errors and uncertainties in the CFD models are addressed. For an extensive insight in this topic refer to [Casey 2000, Versteeg 2007].

The accuracy of a CFD model depends mainly on the following aspects:
- geometry
- meshing
- turbulence model
- boundary conditions
- numerics

The modeled geometry is usually simplified compared to the real device, especially when the model characteristic-length is large compared to small details in the device. How the simplification affects the results plays a major role. Of course the best case is when neglected details are irrelevant for the flow field. This implies a good knowledge of the device fluid-mechanics.

The mesh used for the computation strongly affects the results. Poor quality mesh influences the convergence and the accuracy of the results, as it will be shown in this paper.

The turbulence model and the wall treatment are a further source of uncertainties in the computation. As stated above, their choice is related to assumptions. Since the turbulence and boundary layer behavior in the case of high Re devices is not well understood, it is difficult to assess the impact of the assumptions on the results.

The influence of the boundary conditions on the results is often neglected, mainly assuming constant conditions at inlet and at outlet. Even if at these flow conditions the theoretical necessary length to reach fully developed flow is relatively short (50..100 D, depending on the correlation used), the effect of this assumption on the results has to be evaluated carefully. In large devices such as penstocks, where upstream disturbances influence the flow distribution, short intakes are possible and often the inflow is taken at a free-surface, the definition of the boundary condition can strongly affect the results.

From a numerical point of view, the high Reynolds-number reduces the natural dissipation in the equations, thus making the numerical system more and more unstable. The effect is that small disturbances are not damped and can persist in the flow. Therefore it is more difficult to use an accurate numerical scheme (usually second order), which is prone to over- and undershoots in the solution at large gradients.

Against this effect at least two approaches can be chosen: either use a lower accuracy scheme, such as the Upwind-scheme (first order of accuracy), which, being more diffusive than higher order models introduces in the system numerical dissipation, or switch to unsteady computations. In the first case the computations will more likely converge, but results can be less accurate, whereas the extension of the inaccuracy has to be assessed. In the second case the computations will require an even larger effort (next to the large grid size), thus leading to very high computational time.

SELECTED CASE AND NUMERICAL ASPECTS/PROCEDURE

The investigations were performed with the penstock in Figure 1. The intake is asymmetric and there is an in- plane S-shaped bend between intake and spiral casing.

This case represents a sort of extreme, since the Reynolds number reaches values around 100’000’000.

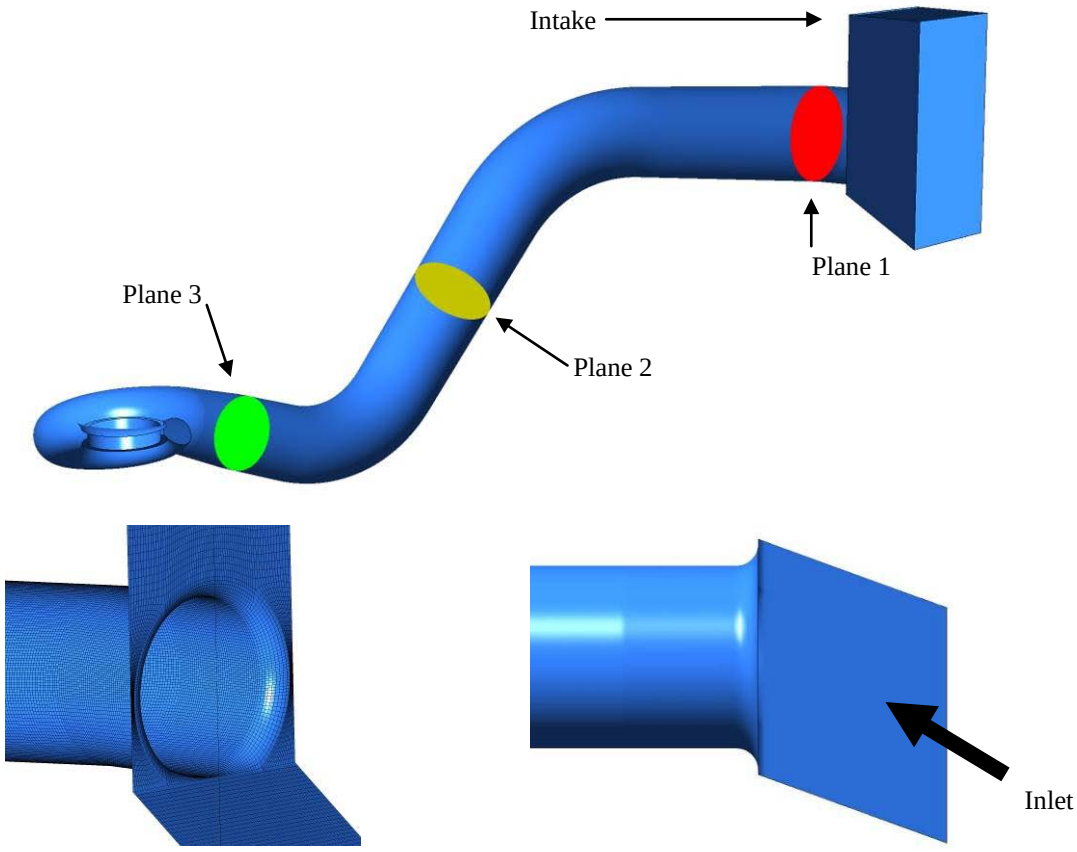

Figure 1: investigated geometry. The three planes used for detailed investigation of the flow distribution are indicated. On the right side a detail of the penstock connection with the intake.

The investigations were preformed with the commercial CFD Package ANSYS CFX V12, a finite volume based code. The structured meshes were created with ANSYS ICEMCFD.

The mesh has 7'000'000 elements. Difficulties in the meshing have been encountered at the junction between intake and the penstock, since the fillet has to be cut in the lower part (see Fig. 1, detail on the right side).

The boundary conditions were defined as follows:

- inlet: total pressure
- outlet: mass flow

The effects of turbulence were computed with a two-equations model, the SST model of [Menter 1994]. The boundary layer at the wall was not explicitly resolved. Instead a universal wall function was used for the computation of the wall shear stress in the first cell.

Computations were performed with two different meshes: one (referred as "mesh 1") generated with usual standard criteria, which results in a rather poor mesh quality for high Reynolds number flows. The critical parts of the mesh are at the beginning and end of the penstock, at the connection with the intake (see Fig. 1) and in the spiral casing. The second mesh (referred as "mesh 2") is an improved mesh, which, as it will be shown, is necessary at the investigated regime.

Three different numerical procedures where used for the investigations:

- first order (upwind) steady state spatial discretisation
- formal second order steady state discretisation
- formal second order unsteady state discretisation

The choice is taken in order to show the influence of the numerical schemes on the solution itself and its convergence.

RESULTS

Two comparisons will be shown

- "mesh 1" and "mesh 2" for first and second order steady schemes
- "mesh 2" with second order steady vs. standard mesh with second order unsteady scheme

As a reference quantity the axial velocity distribution on plane 3 is taken (see Fig. 1), this being also the relevant quantity for the mass flow integration. In Figure 2 the velocity vectors for the secondary flow are also depicted. Considering the convergence of the cases, it can be said that the case with second order scheme for steady flow and standard quality mesh did not converge, with the maximum of the normalized residuum not below 3e-2. All the other cases reached a good to very good convergence, where the cases with high quality mesh show the maximal residuum below 1e-5 and the RMS residuum at least two orders of magnitude lower.

Starting the analysis with the first order scheme, it can be seen that the solution is practically the same for both meshes, thus underlining the common experience in usual applications, that the high numerical diffusivity typical of a first order scheme can overcome shortcomings in the mesh quality.

On the other end it can be seen that the change due to the mesh observed for the second order steady-scheme is very clear, showing that special care for the mesh quality is mandatory for steady state computations at very large Reynolds numbers.

A possibility to reach converged results with the standard mesh but still using a second order scheme is to switch to the unsteady mode. The unsteady procedure forces convergence at every iteration using inner loops, thus alleviating the mesh problems, which are in most of the cases given by non-orthogonality in parts of the mesh. A clear disadvantage of this procedure is the large increase of computational time (every iteration performs multiple inner loops, usually about 10) needed to reach convergence.

Using a dual strategy for convergence, the process can be significantly accelerated. In a first phase a rather large time step has to be chosen, in order to let the main flow adjust to a satisfactory guess. In a second phase the time step has to be reduced in order to reach the final solution. Nevertheless the effort is much larger than that needed for a steady state computation on a high quality mesh.

As a final comparison, the first and second order results on the improved mesh are compared. The difference is quite substantial, especially in the boundary-layer thickness at the wall. The stagnation points due to the secondary flow are at different positions, as well as the main vortices at the center of the cross section.

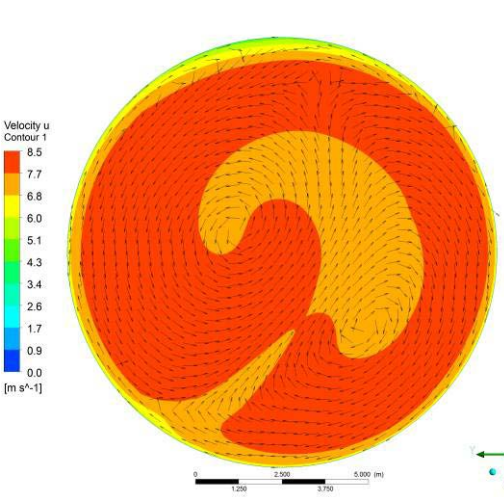

Standard mesh, first order scheme

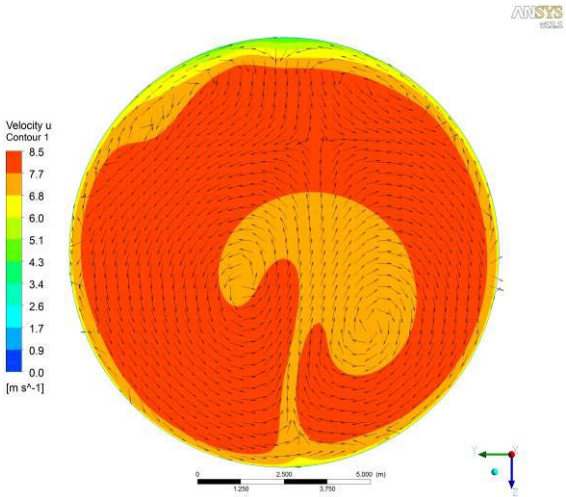

Standard mesh, second order scheme steady

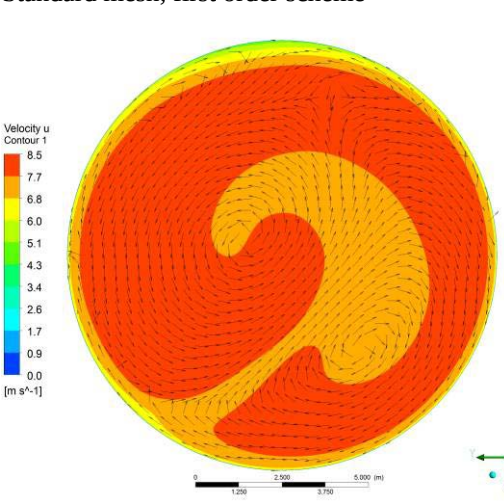

Improved mesh, first order scheme

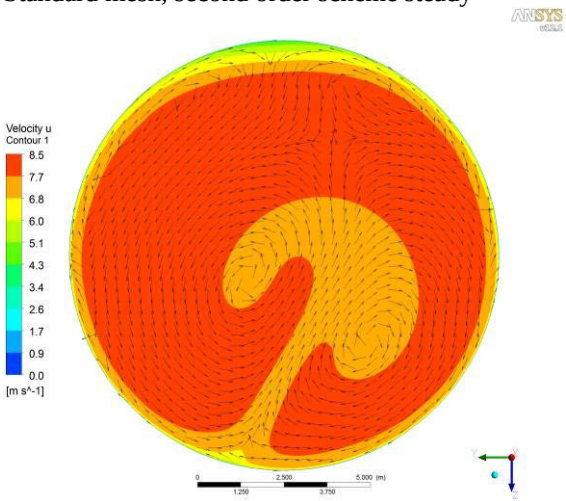

Improved mesh, second order scheme steady

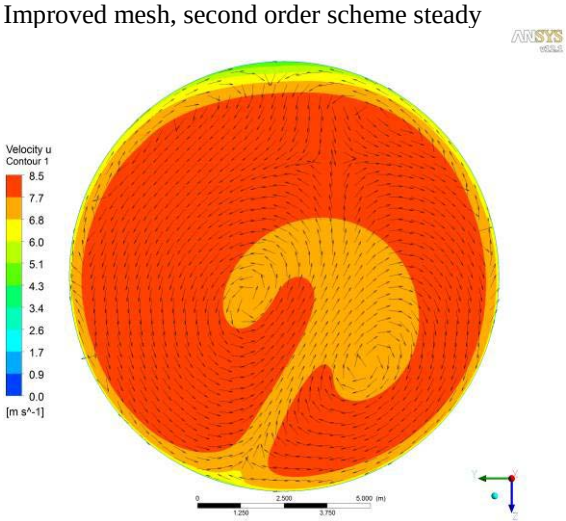

Standard mesh, second order scheme unsteady

Fig. 2: Axial velocity distribution at plane 3

COMMENTS ON THE FLOW PHYSICS

The flow physics in the pipe is discussed using the distribution of selected quantities at plane 1, 2 and 3. Only the results for the improved mesh are shown, emphasizing the difference on the chosen numerical scheme.

Fig. 3 shows the axial velocity distribution in the penstock in plane 1 (after the intake) and plane 2 (after the first bend). The overall picture is the same for both numerical schemes, showing in the lower part of the section the core of the flow and a thick boundary layer at the top. Looking more carefully at some details the typical behavior of the numerical schemes can be detected. The thickness of the boundary layer is in general much larger for the first order scheme, which tends to diffuse the influence of the wall into the flow field. Moreover on the left part of the section there is a disturbance coming from the asymmetrical intake. While the first order scheme smears it out and at this position is almost no more present, the second order solution tends to preserve it.

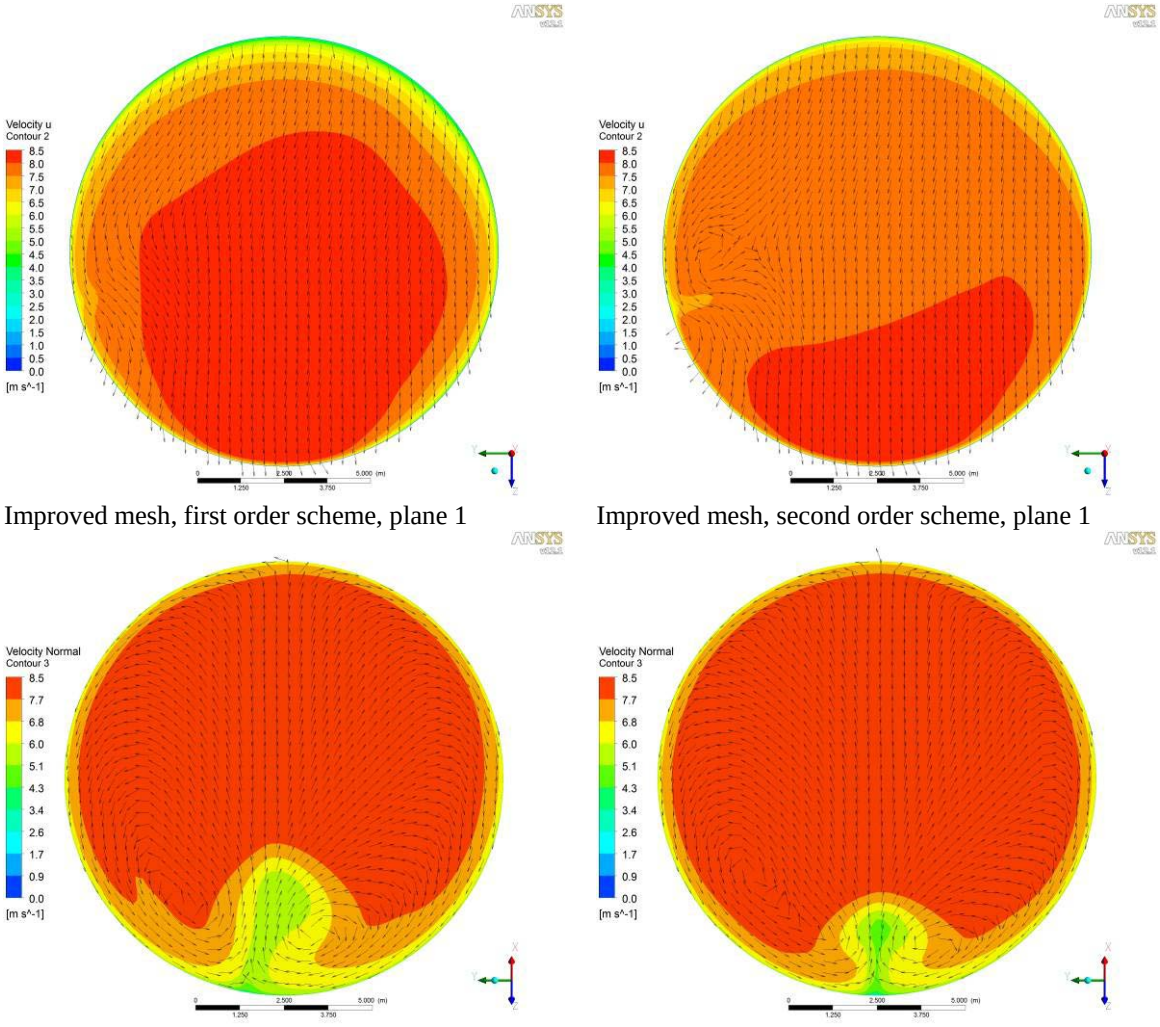

Improved mesh, first order scheme, plane 1 — Improved mesh, second order scheme, plane 1

Improved mesh, first order scheme, plane 2 — Improved mesh, second order scheme, plane 2

Fig. 3: Axial velocity distribution along the penstock (plane 1 and plane 2).

Further down at plane 2, after the first bend, the typical secondary flow structure with a double vortex is detected. Due to the bend in the penstock, which produces a pressure gradient in the section pointing upward (high pressure on the outside of the bend), the boundary layer flow is moved toward the low pressure region and gathered at the bottom of the section.

Both schemes present a similar flow behavior, but with clear differences. Since the boundary layer development in the first part of the penstock was stronger for the first order case (due to numerical effects), the low velocity region at plane 2 is for this scheme much larger than for the second order scheme.

It is interesting to note that on the upper part of the section a “new” boundary layer is formed, which is similar in extent for both cases.

The next bend in the penstock produces a pressure gradient in the opposite direction compared to the previous one, thus pointing downwards. The low momentum water, in the newly formed boundary layer and on the bottom of the section, can not balance the gradient imposed by the flow in the core, and starts to move upwards. The boundary layer flow produces a flow sheet at the wall moving also upwards, in the opposite direction of the main secondary flow, while the low momentum fluid at the section’s bottom drifts towards the center of the penstock.

These secondary flow movements are shown in Fig. 4, where the vertical velocity in the section is depicted: red pointing downwards and blue upwards, respectively. Regarding the numerics, the main features of the secondary flow are captured by the first order scheme in a similar way as the second order scheme does.

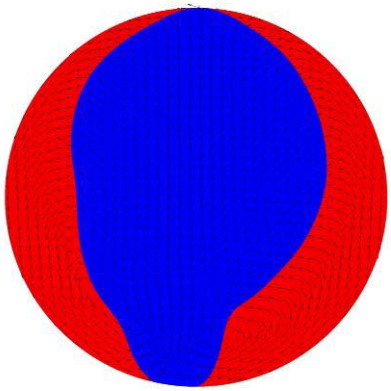

Improved mesh, first order scheme, plane 2

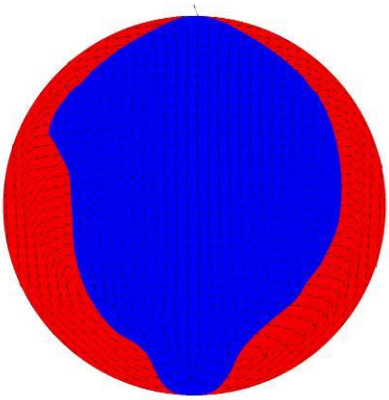

Improved mesh, second order scheme, plane 2

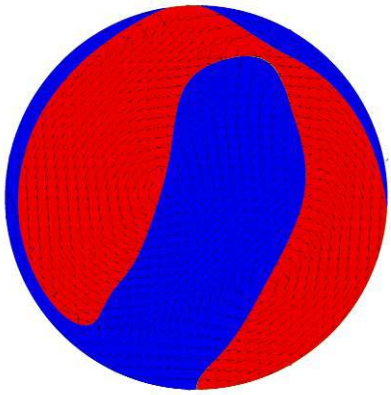

Improved mesh, first order scheme, plane 3

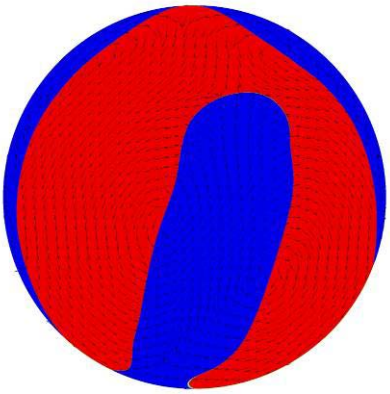

Improved mesh, second order scheme, plane 3

Fig. 4: In-plane velocity distribution along the penstock (plane 2 and plane 3). Red: secondary flow moving downwards in the section, blue upwards.

Fig. 5 shows the velocity distribution on a vertical and horizontal line on plane 3. It is quite clear that the disturbances introduced by the asymmetric intake and the S-shaped penstock are large and have a three-dimensional character. The low momentum flow accumulated after the first bend is displaced by the second bend toward the center of the section and is clearly noticeable in the velocity profiles.

The disturbed velocity profile can be handled at least with two different approaches in order to minimize the integration error:

- use of adaptive OWICS, having the benefit of dynamic adjustment of the flow parameters [Ref. Gruber 2010]
- increase the number of acoustic paths.

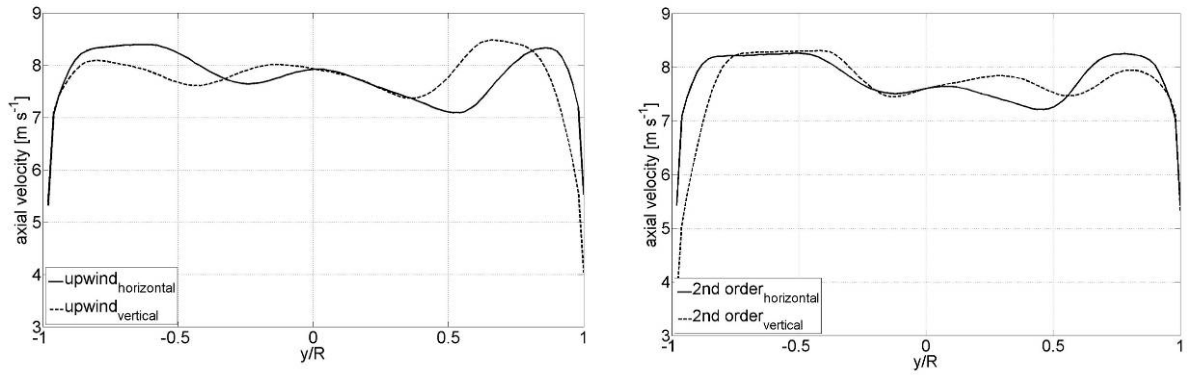

Improved mesh, first order scheme, plane 3 Improved mesh, second order scheme, plane 3

Fig. 5: Axial velocity distribution along a horizontal (left) and a vertical line (right) at plane 3.

The first approach gives usually good results already when using 4 acoustic paths. It is mainly suited when a disturbed but symmetric distribution is present. In this case, due to the asymmetric intake, the flow distribution is uneven, which can lead to even larger errors in the mass flow integration than a standard OWICS [Gruber 2010].

Therefore it has to be assessed if through a particular positioning of the paths, whether aligned with or perpendicular to the disturbance, a more or less symmetric velocity-distribution can be seen by the sensors.

The last choice, where the number of paths has to be increased in order to capture the effects of the strong disturbances, is also the most expensive one.

CONCLUSIONS

The flow in a large Reynolds-number penstock has been computed with different numerical parameters. The influence of mesh quality, numerical scheme and simulation type (steady or unsteady) is presented. The mesh plays a key role for convergence and special care should be taken during the grid generation process. The shortcomings due to the use of a low quality mesh can be overcome with numerical dissipating schemes, like a first order scheme (also known as upwind scheme), or with unsteady computations, which compensate the problems in the mesh with a large number of inner loops and thus lead to a considerable increase in computational time.

The results in the in-plane S-shape penstock show a complicated secondary flow pattern. After the first bend, low momentum flow from the boundary layer is gathered at the low pressure (i.e. inner) side of the penstock bend. The successive bend, producing an opposite pressure gradient, displaces the low momentum flow toward the section center, thus leading to a velocity distribution with a low velocity in the penstock center. At the same time the new boundary layer flow is forced to move against the pressure gradient. For discharge measurements this means that particular care in the method selection has to be applied.

REFERENCES

1. Marusic et al., 2010, “Wall-bounded turbulent flows at high Reynolds numbers: Recent advances and key issues”, PHYSICS OF FLUIDS 22, 065103.

2. T. Staubli et al., 2007, “CFD optimized acoustic flow measurement and laboratory verification”, HYDRO 2007, Granada, Spain.

3. T. Staubli et al., 2008, ”Optimization of acoustic discharge measurement using CFD“, Hydropower & Dams, Issue Two, 2008.

4. A. Adamkowski et al., 2008, “Flow rate measurement using the pressure-time method in a hydropower plant curved penstock”, IGHEM 2008, Milano.

5. F.R. Menter, 1994, “Two-equation eddy-viscosity turbulence models for engineering applications”, AIAA-H.K. M. Casey et al., 2000, “Quality and Trust in Industrial CFD“, ERCOFTAC Best Practice Guidelines Journal, 32(8), pp. 1598 - 1605.

6. H. K. Versteeg, W. Malalasekera, “An introduction to computational fluid dynamics”, Pearson Prentice Hall, Second Edition 2007.

7. P. Gruber et al., 2010, Optimization of the ADM by Adaptive Weighting for the Gaussian Quadrature Integration, IGHEM 2010, Roorkee.